Proc. NIPR Symp. Upper Atmos. Phys., 12, 131–137, 1998

VERTICAL ATTENUATION RATE OF ATMOSPHERIC GRAVITY WAVES IN THE LOWER-*F* REGION OBSERVED WITH THE EISCAT RADAR (EXTENDED ABSTRACT)

Takashi SHIBATA[1], Ryoichi FUJII[2] and Kristian SCHLEGEL[3]

[1] *University of Electro-Communications, Chofugaoka, Chofu-shi, Tokyo 182-8585*
[2] *Solar-Terrestrial Environment Laboratory, Nagoya University, Furo-cho, Chikusa-ku, Nagoya 464-8601*
[3] *Max-Planck-Institut für Aeronomie, Max-Planck-Straße 2, D-37191 Katlenburg-Lindau, Germany*

Atmospheric gravity waves (AGWs) are believed to play an important role in the transportation and redistribution processes of excess energy in the upper atmosphere. Much of the experimental evidence of the existence of AGWs at ionospheric heights has been derived using a variety of radio techniques, *e.g.*, HF Doppler, ionosonde, Faraday rotation, meteor radar and incoherent scatter radar (ISR) (see, for example, the reviews by HUNSUCKER (1982) and HOCKE and SCHLEGEL (1996), and references therein). From these observational studies, our knowledge of the morphology of AGW occurrence and AGW propagation in the ionosphere has been considerably advanced. Nowadays, major interest is to be directed to problems concerning the energy budget in the thermosphere, i.e., the vertical structure and the power profile of AGWs.

The height-dependent AGW parameters in the high-latitude region have been investigated with the data of ISR. Recently, NATORF *et al.* (1992) have derived the vertical wavenumber of AGWs by applying a height-dependent inversion technique to the ion velocity data obtained with the EISCAT radar and suggested that $\boldsymbol{E}\times\boldsymbol{B}$ drift and vertical neutral winds might contribute to the AGW vertical propagation and its energy loss. The AGW activities in the *F*-region have been studied in detail by LANCHESTER *et al.* (1993) using coincident and co-sited measurements from EISCAT and Dynasonde, and the horizontal and vertical wavelengths have been determined by solving the Hines dispersion equation (HINES, 1960) incorpolated with the observed frequency, field-aligned wavelength and the background neutral wind. SHIBATA and SCHLEGEL (1993) have investigated the vertical structure of AGW activity by using the ion temperature data of EISCAT and concluded that the essential feature of the power variation can be explained in terms of the energy conservation of AGWs propagating in a dissipative thermosphere.

The purpose of this paper is to present the results of further analysis on the vertical attenuation rate of AGWs in the *E* and lower-*F* regions by taking advantage of the capability of EISCAT to cover a wide height range with a good range resolution. In the present analysis, we used the data from the Tromsø (69.59°N, 19.23°E) measurements in the common programme 1 (CP1) observation mode, which cover the altitude range from about 90 to 268 km, nearly along the geomagnetic field line, with a resolution of about 3 km in height and 5 min in time.

The AGW associated fluctuation in the ionospheric plasma parameters has, in

Table 1. Summary of the data set we analyzed.

Date	Time (UT)	Height (km)	Planetary 3-hour-range index K_p								
			1	2	3	4	5	6	7	8	Sum
310792	0500–1700	101–250	2	1	2	2	2	3	2	4	18
020892	1100–1700	101–250	1	1	1	1	1	1	2	2	10
030892	0500–1700	101–250	1	1	1	1	1	1	2	1	8
040892	0500–1200	101–250	2	1	1	1	3	4	5	3	21

general, a relatively small amplitude. Reliability of the fluctuation analysis is therefore strongly dependent on the signal-to-noise ratio (*SNR*) of the observations. We have restricted our analysis to the data of daylight hours in which the *SNR* takes relatively high values owing to the high electron density. The data below 100 km are occasionally affected by *SNR* limitations. In order to remove such effects, we used the data between the altitudes of 100 and 250 km.

In the high-latitude ionosphere, the contamination of AGW signatures by electrodynamical effects, for example, by electric field and particle precipitation, is a serious problem. Sometimes such local effects can hardly be distinguished from the AGW associated fluctuations. In order to avoid the contamination of possible local effects in the detection of AGW activity, the present analysis is restricted to the data taken during low geomagnetic activity ($K_p \leqq 3$). Summary of the 4 day data set we analyzed is listed in Table 1.

The reaction of ionization to AGW passage is found to be very complex in general and dependent on plasma parameters (KLOSTERMEYER, 1969; SHIBATA, 1983; KIRCHENGAST *et al.*, 1995, 1996; HOCKE *et al.*, 1996). In the case of low geomagnetic activity, the effects of ionospheric electric field, and hence the effects of frictional heating on the ionic constituents can be accepted to be negligibly small. In such a case, theory tells us that the ion temperature (T_i) will be a very good estimate of the neutral temperature in the E- and lower F-region altitudes (SCHUNK, 1975). In the present analysis, therefore, we use just the T_i data to detect the AGW activities.

In order to investigate the fluctuation properties quantitatively, we have provided the fractional variations, $dT_i/T_{i,0}$, of the measured ion temperature by removing the base value $T_{i,0}$ from the raw data at each altitude. The base value has been assumed to be composed of the d.c. component and 24-, 12-, 8- and 6-hour tidal harmonics:

$$T_{i,0}(t) = T_{i,\mathrm{d.c.}} + \sum_{k=1}^{4} A_k \cos\left(\frac{2\pi kt}{24} - \phi_k\right), \tag{1}$$

where the d.c. component $T_{i,\mathrm{d.c.}}$ and the amplitude A_k and phase ϕ_k of the k-th harmonic are calculated by least squares fit to the raw data. Figure 1 shows an example of a time-altitude-intensity plot of the $dT_i/T_{i,0}$ fluctuations observed on 31 July 1992. The solid (dotted) line contours denote positive (negative) values, and the contour step is 2% in the fractional magnitude. The display after about 1800 UT is omitted because the fluctuation properties seem to be strongly influenced by some possible local effects. The horizontal arrow beside the axis of abscissa denotes the data period we analyzed. We can easily find the AGW associated fluctuations showing a forward phase progression

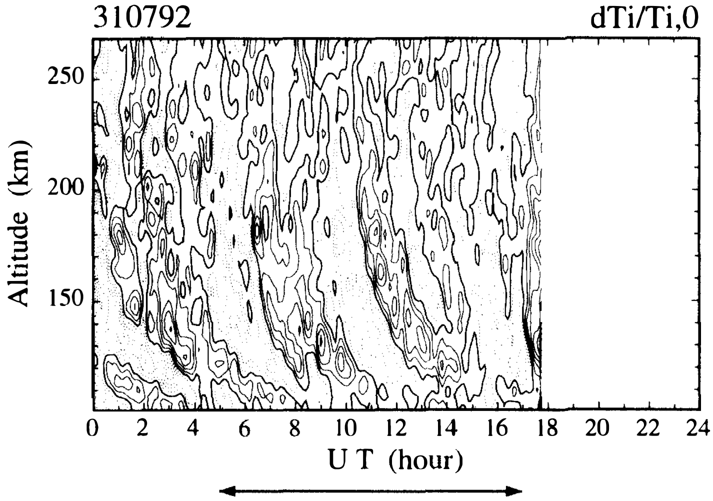

Fig. 1. Contour plot of the fractional ion temperature fluctuations observed on 31 July 1992. The solid (dotted) line contours denote positive (negative) values. The contour step is 2% in the fractional magnitude.

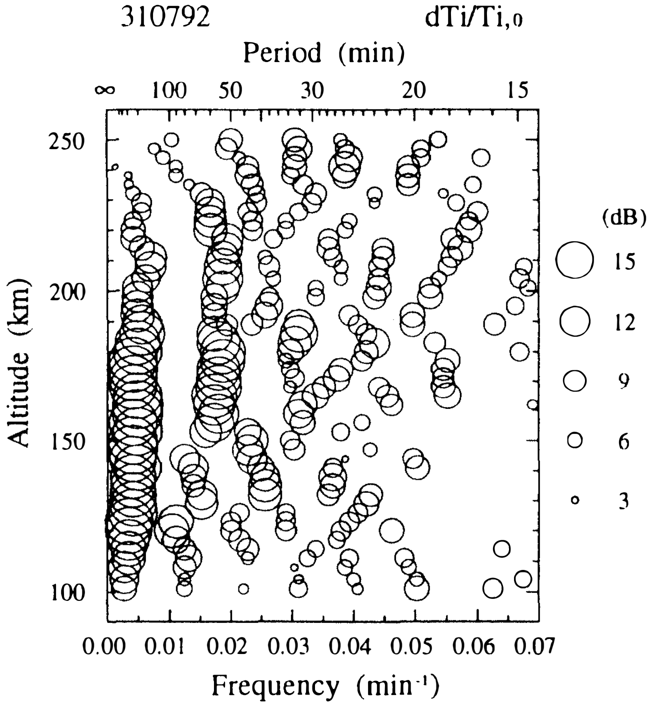

Fig. 2. Spectral peak distribution vs altitude for the ion temperature fluctuations observed on 31 July 1992. The center of each circle denotes the position of spectral peak in the frequency-altitude frame and the radius of each circle is proportional to the relative magnitude (in dB) of power spectral density with respect to the background level.

with decreasing altitude, which means an AGW carrying energy upward.

The dominant component of $dT_i/T_{i,0}$ fluctuation was identified by carrying out the spectrum analysis in each altitude gate. Maximum entropy method (MEM) was used to obtain high-resolution power spectra. Figure 2 shows a result of spectrum analysis obtained from the data during 0500–1700 UT of 31 July 1992. The center of each circle denotes the position of spectral peak in the frequency-altitude frame, and the radius of each circle is proportional to the logarithm of the relative magnitude of power spectral density with respect to the background level. Following the method of SHIBATA and SCHLEGEL (1993), the background power level is obtained from the trend of the minimum value of each spectral component in the whole altitude range of analyses. The spectral peaks are displayed up to a frequency of 0.07 min^{-1} (about 14 min in period) where the spectral power has already become extremely low. It is also to be noted that the results in the frequency range less than about 0.0028 min^{-1} (360 min period) are meaningless, since we have used a sort of high-pass filter in the process of base value removal from the raw data.

It will be seen from Fig. 2 that the intensity as well as frequency of the dominant spectral component depends on the altitude. In order to discuss the altitude variation of the AGW activity more quantitatively, we have traced the spectral peak in the frequency-altitude frame and obtained the spectral power varation against the altitude for several dominant components as shown by thin lines in Fig. 3, where the solid, dot-dashed, broken and dotted lines denote the components with the period around 181, 67, 44 and 35 min, respectively. The abscissa represents the spectral power integrated over the frequency interval between two neighbouring spectral minima on both sides of the specified spectrum peak. Although the absolute value of the spectral power in the MEM estimate does not reflect the true power, LACOSS (1971) has proven in his numerical experiments that the integrated MEM power varies only from 90 to 99% of the correct value. In the procedure of spectral peak tracing, we have allowed any data

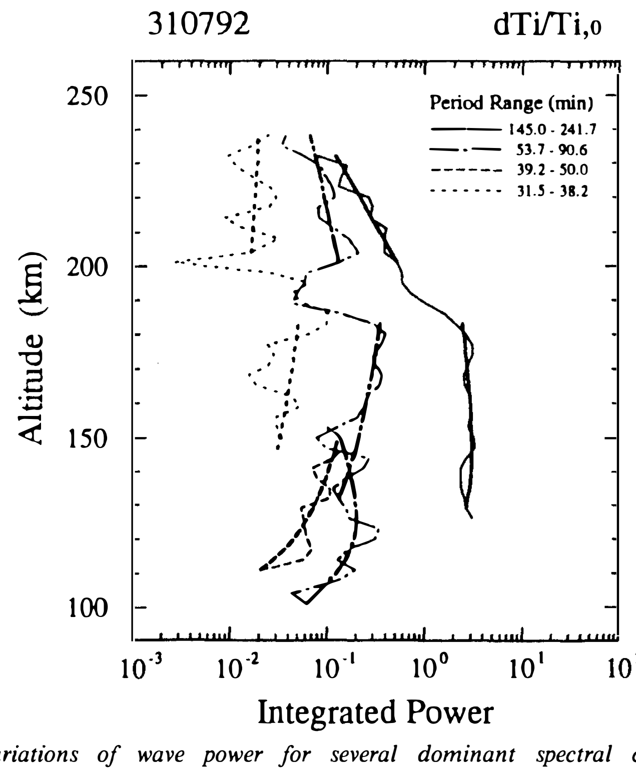

Fig. 3. Altitude variations of wave power for several dominant spectral components; the solid, dot-dashed, broken and dotted lines denote the components with the period around 181, 67, 44 and 35 min, respectively. For the meaning of the the thick lines, see text.

gap within the length of 2 successive altitude gates (about 6 km), because the vertical wavelength of a typical AGW has been accepted to be in the order of 100 km (*e.g.*, MORGAN and TEDD, 1983). As is well-known, the AGW propagation is strongly influenced from the prevailing neutral wind, which has a complex profile depending on the time, altitude, activity, *etc.*, with typical horizontal speed reaching up to the order of 100 m/s (*e.g.*, BREKKE *et al.*, 1995). If we assume the horizontal wavelength of 1000 km (*e.g.*, MORGAN and TEDD, 1983; SHIBATA and SCHLEGEL, 1993), the amount of Doppler shift due to the background neutral wind in the observed frequency has been estimated to be 3–4% at least for the AGW of 360 min period. The amount of frequency shift for the shorter period AGWs will be expected to be more large, because the wavelength tends to decrease with a decrease in wave period. The frequency difference between traceable spectral peaks at successive altitude gates, therefore, has been restricted within 1% of the specified frequency. Finally, the successions of spectral peaks continuing over 30 km in the vertical direction have been selected for the following analyses.

The thick lines in Fig. 3 are the fitted curves to each power profile obtained by the least squares method and the assumption that the wave power variation are to be expressed by a monochromatic plane-wave type equation in a stratified dissipative thermosphere with the form,

$$\propto \exp\left[-2\int_{z_1}^{z_2}\left(\widetilde{k_z^i}-\frac{1}{2H}\right)dz\right]. \tag{2}$$

Here, z is the altitude, $\widetilde{k_z^i}$ the effective attenuation rate of wave amplitude in the vertical direction for a specified spectral component, and H the locally defined scale height of the neutral atmosphere calculated from the MSIS86 model. It can be seen from this figure that the essential feature of the wave power variation is highly consistent with that of AGWs in a stratified dissipative thermosphere eq. (2) with exception at altitude range of

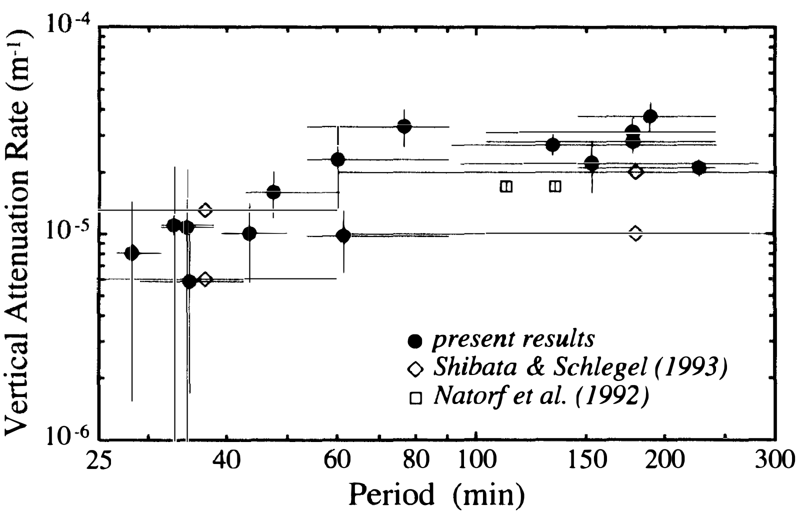

Fig. 4. Period dependence of the vertical attenuation rate of observed AGWs. The bold circles denote the present results, and the open diamonds and squares are from the results of SHIBATA *and* SCHLEGEL *(1993) and* NATORF *et al. (1992), respectively. The horizontal and vertical bars represent the deviations of estimate.*

180–200 km.

The resultant fitted values of $\widetilde{k_z^i}$ obtained from the 4 day data set are plotted against the wave period in Fig. 4 by bold circles. The horizontal bar denotes the range between minimum and maximum periods of the specified spectral component, and the vertical bar represents the deviation of $\widetilde{k_z^i}$ value which has been estimated from the fitting error. The results of the earlier investigations made by NATORF *et al.* (1992) and SHIBATA and SCHLEGEL (1993) are also plotted by open squares and diamonds, respectively. It can be seen from this figure that (1) the present results are almost consistent with those of the earlier investigators, and (2) the value of $\widetilde{k_z^i}$ has a tendency to increase with an increase in wave period. The latter issue agrees well with the theoretical prediction of AGW dissipation in a realistic thermosphere model (KLOSTERMEYER, 1972; SHIBATA, 1983).

In the case of Fig. 3, the fit to the portion of $z \simeq 180$–200 km could not be accomplished with any resonable value of $\widetilde{k_z^i}$. The altitude region of such a rapid power variation, probably connected with a much higher value of $\widetilde{k_z^i}$, varies on a case-by-case basis in the present data set we analyzed. We cannot regard these drastic energy losses as a consequence of the ordinary energy dissipation of AGWs alone. For such a rapid decrease in the AGW power, SHIBATA and SCHLEGEL (1993) have pointed out a possible connection with the transition of the dominant component in the wind variation (from semidiurnal to diurnal). Futher investigation of the AGW activity and its possible relation with the prevailing wind field is left for the subject of energy budget in the thermosphere in our future work.

Acknowledgments

We are indebted to the Director and staff of EISCAT for operating the facility and supplying the data. EISCAT is an International Association supported by Finland (SA), France (CNRS), the Federal Republic of Germany (MPG), Japan (NIPR), Norway (NFR), Sweden (NFR) and the United Kingdom (PPARC). The data archives have been made at Solar-Terrestrial Environment Laboratory, Nagoya University.

References

BREKKE, A., NOZAWA, S. and SATO, M. (1995): Samples of auroral *E*-region parameters derived from EISCAT experiments. J. Geomagn. Geoelectr., **47**, 889–909.

HINES, C. O. (1960): Internal atmospheric gravity waves at ionospheric heights. Can. J. Phys., **38**, 1441–1481.

HOCKE, K. and SCHLEGEL, K. (1996): A review of atmospheric gravity waves and travelling ionospheric disturbances: 1982–1995. Ann. Geophys., **14**, 917–940.

HOCKE, K., SCHLEGEL, K. and KIRCHENGAST, G. (1996): Phases and amplitude of TIDs in the high latitude *F*-region observed by EISCAT. J. Atmos. Terr. Phys., **58**, 245–255.

HUNSUCKER, R. D. (1982): Atmospheric gravity waves generated in the high-latitude ionosphere: A review. Rev. Geophys. Space Phys., **20**, 293–315.

KIRCHENGAST, G., HOCKE, K. and SCHLEGEL, K. (1995): Gravity waves determined by modeling of traveling ionospheric disturbances in incoherent-scatter radar measurements. Radio Sci., **30**, 1551–1567.

KIRCHENGAST, G., HOCKE, K. and SCHLEGEL, K. (1996): The gravity wave–TID relationship: Insight via theoretical model–EISCAT data comparison. J. Atmos. Terr. Phys., **58**, 233–243.

KLOSTERMEYER, J. (1969): Gravity waves in the *F*-region. J. Atmos. Terr. Phys., **31**, 25–45.

KLOSTERMEYER, J. (1972): Numerical calculation of gravity wave propagation in a realistic thermosphere. J. Atmos. Terr. Phys., **34**, 765–774.

LACOSS, R. T. (1971): Data adaptive spectral analysis method. Geophysics, **36**, 661–675.

LANCHESTER, B. S., NYGRÉN, T., JARVIS, M. J. and EDWARDS, R. (1993): Gravity wave parameters measured with EISCAT and Dynasonde. Ann. Geophys., **11**, 925–936.

MORGAN, M. G. and TEDD, B. L. (1983): The dispersion of traveling ionospheric disturbances. J. Geophys. Res., **88**, 10253–10258.

NATORF, L., SCHLEGEL, K. and WERNIK, A. W. (1992): Gravity wave parameters derived from traveling ionospheric disturbances observations in the auroral zone. Radio Sci., **27**, 829–840.

SCHUNK, R. W. (1975): Transport equations for aeronomy. Planet. Space Sci., **23**, 437–485.

SHIBATA, T. (1983): A numerical calculation of the ionospheric response to atmospheric gravity waves in the *F*-region. J. Atmos. Terr. Phys., **45**, 797–809.

SHIBATA, T. and SCHLEGEL, K. (1993): Vertical structure of AGW associated ionospheric fluctuations in the *E*- and lower *F*-region observed with EISCAT–A case study. J. Atmos. Terr. Phys., **55**, 739–749.

(Received December 1, 1997; Revised manuscript accepted January 27, 1998)